JOURNAL OF SPACECRAFT AND ROCKETS
Vol. 42, No. 1, January–February 2005

Preliminary Design of Earth–Mars Cyclers Using Solar Sails

Robert Stevens* and I. Michael Ross†
Naval Postgraduate School, Monterey, California 93943

Motivated by the concept of using cycler trajectories for Mars return missions, an optimal Earth–Mars cycler is designed for spacecraft that use solar sails. The design is preliminary in the sense that the trajectories are assumed to be coplanar and the orbits of Earth and Mars are assumed to be circular. The optimality criterion is the vehicle's hyperbolic excess speed V_∞ with respect to Mars. This trajectory optimization problem is formulated using the framework of optimal periodic control with interior point constraints that include jump discontinuities that arise as a result of gravity assists. The problem is numerically solved using the concept of pseudospectral knots (PSK) by way of a general-purpose dynamic optimization software. Feasibility of the PSK-derived trajectories is demonstrated using numerical propagation. Results show that solar sails can be used to reduce significantly V_∞ at Mars. For example, it is shown that a sail with a lightness number of 0.17 can achieve a V_∞ with respect to Mars of 2.5 km/s at every synodic encounter.

Nomenclature

c	=	speed of light, m/s
D	=	hyperbolic periapse distance from center of a planet, normalized by R
$\boldsymbol{e}$	=	events function
m	=	mass of spacecraft, kg
n	=	mean motion of planet, rad/time unit (TU), where $2\pi\,\mathrm{TU} = 1$ year
R	=	radius of planet, km
r	=	magnitude of $\boldsymbol{r}$, astronomical unit, AU
$\boldsymbol{r}$	=	radius vector from the sun, AU
t	=	time, TU
u	=	radial velocity magnitude
$\boldsymbol{V}$	=	velocity of spacecraft in heliocentric frame, AU/TU
$\boldsymbol{V}_\infty$	=	hyperbolic excess velocity with respect to planet, AU/TU
V_∞	=	hyperbolic excess speed, AU/TU
v	=	transverse or along-track velocity magnitude, AU/TU
$\boldsymbol{x}$	=	state vector for spacecraft
α	=	solar sail cone angle, rad
β	=	solar sail lightness number
δ	=	gravity-assist deflection angle or turn angle, rad
ζ	=	Earth–Mars lead angle, rad
θ	=	spacecraft angular displacement in ecliptic, rad
μ	=	gravitational parameter of sun, $\mathrm{AU}^3/\mathrm{TU}^2$
ϕ	=	Mars's angular displacement (mean anomaly), rad
ψ	=	Earth's angular displacement (mean anomaly), rad

Subscripts

$0, i, f$	=	initial, intermediate, or final conditions, respectively
e, m, p	=	Earth, Mars, or planet, respectively

Superscripts

$-, +$	=	immediately before or following an interior event, respectively
$\cdot$	=	time derivative of a given variable
$\wedge$	=	unit vector direction

Presented as Paper AAS 2003-244 at the AAS/AIAA 13th Space Flight Mechanics Meeting, Ponce, PR, 9–13 February 2003; received 7 June 2003; revision received 9 March 2004; accepted for publication 9 March 2004.

*Graduate Student, Department of Aeronautics and Astronautics; resteven@nps.navy.mil. Student Member AIAA.

†Associate Professor, Department of Aeronautics and Astronautics, Code AA/Ro; imross@nps.navy.mil. Associate Fellow AIAA.

Introduction

WITH ongoing interest in Mars missions, there has been considerable attention devoted to developing space trajectories that make regular repeated passes of our neighboring planet and our home planet.[1–5] These trajectories, known as cyclers, could be tremendously valuable for missions ranging from sample returns to ferrying supplies and personnel between the planets like escalators. Naturally occurring cycler trajectories would be ideal, requiring no added energy other than that provided by the gravity fields of the target planets. If such "free ride" paths exist, they could host shuttling spacecraft making an infinite number of round trips without requiring propulsion systems. This hypothetical path would be characterized by natural motion that repeats itself endlessly. In this paper, we focus on Earth–Mars cyclers. To this end, two prominent proposals for such Earth–Mars cyclers have been proposed: the Aldrin cycler (see Ref. 4) and the Versatile International Station for Interplanetary Transport (VISIT) 1 and 2 cyclers.[5] The Aldrin cycler uses gravity assists from both planets and small well-timed course adjustment maneuvers to maintain a continuous cycling trajectory. Although the revisit times are appealing (7 round trips in 15 years), onboard propellant is required to provide a cumulative ΔV of approximately 2 km/s for a 15-year mission. Because no propellant is expended trying to reduce speed in the vicinity of a target planet, approach speeds are high (6.54 km/s at Earth and 9.75 km/s at Mars). A VISIT cycler, on the other hand, uses neither gravity assists nor propellant for ΔV burns for orbit shaping, but rather resides in a natural heliocentric orbit that makes regular passes of both Earth and Mars. The advantage to this cycler is that no propellant is required to maintain the orbit for up to 20 years, but the primary disadvantages are that there are rather long revisit times and that large approach distances are needed to minimize planetary gravitational interaction. For the VISIT 1 cycler, three Earth visits and four Mars visits occur every 15 years.

The purpose of this paper is to present an Earth–Mars cycler concept using solar sails[6] that has the advantages of both cyclers without the expense of onboard propellant. See Refs. 6 and 7 and the references contained therein for an extensive discussion on solar sailing. It has been shown that a nearly ballistic cycler orbit can be maintained for 15 years; thus, it is reasonable to speculate that a solar sail cycler is not only feasible, but more capable because it provides free controls by way of the sun's inexhaustible source of energy. With solar radiation pressure providing free thrust to the solar sail, a cycler orbit may be maintained with short revisit times, as well as slow planetary approach speeds. Small approach velocities to Earth and Mars at short distances are desirable for operational reasons and because they exhibit attractive orbit-shaping characteristics due

to large angle gravity-assist maneuvers. This concept is explored in this paper. Results are preliminary in the sense that two-dimensional trajectories are considered. A further simplification adopted in this paper is the modeling of gravity assists. Planetary gravity assists are modeled as instantaneous changes in the velocity vector with the resulting ΔV being constrained by two-body orbital mechanics (between the spacecraft and the planet). Under these simplifications, the cycler problem can be posed as an optimal periodic control problem with constrained state discontinuities at interior points. This problem is solved using the concept of pseudospectral knots[8–10] by way of the general-purpose dynamic optimization software package DIDO.[11] See Refs. 8–11 for theoretical and computational details on the trajectory optimization method.

Sail Model

A solar sail is a very large thin lightweight structure that transfers momentum from inbound solar photons to the spacecraft.[6] Thus, for a maximum transfer of momentum, the sail must be made of a highly reflective material (ideally, with unity reflectivity). For this analysis, the sail is modeled as a flat film (nonbillowing sail) with a one-sided perfectly specular-reflecting surface. To characterize sail performance, we use the sail lightness number β, defined as the ratio of the acceleration from solar radiation pressure to the acceleration from the sun's gravity (Ref. 6, pp. 38–40),

$$\beta = a_{\text{srp}}/a_{\text{grav}} = \left[\left(2W_e r_e^2/mc\right)A\right]/\mu \tag{1}$$

where W_e is the solar energy flux at 1 AU, r_e is the sun–Earth distance, A is the sail area, and μ is the solar gravitational parameter. Both accelerations are proportional to the inverse square of the radial distance from the sun, and so β is an apt indicator of sail performance independent of location. For this paper, a lightness number of $\beta = 0.17$ was used to model a reasonably high-performance solar sail consistent with prior studies.[6,12]

The sail control angle α, called the cone angle, is defined as the angle between the sun sail position vector $\boldsymbol{r}$ and the sail normal $\boldsymbol{n}$ (Fig. 1). This angle determines both the magnitude and direction of a solar force imparted to the spacecraft. For a single-sided sail, the control angle is bounded by

$$-\pi/2 \le \alpha \le \pi/2 \tag{2}$$

Dynamics Model

Because only coplanar orbits are considered in this analysis, we employ a two-dimensional dynamic model with the sail cone angle as the control. When polar coordinates are used in the heliocentric frame, the equations of motion for the state vector $\boldsymbol{x} = [r, \theta, u, v]^T$ with control α are (Refs. 6, p. 118, and 12)

$$\dot{r} = u, \qquad \dot{\theta} = v/r, \qquad \dot{u} = v^2/r - \mu/r^2 + (\beta\mu/r^2)\cos^3\alpha$$
$$\dot{v} = -uv/r + (\beta\mu/r^2)\cos^2\alpha\sin\alpha \tag{3}$$

where r, θ, u, and v and are the radial distance, angular displacement, radial velocity, and transverse velocity, respectively.

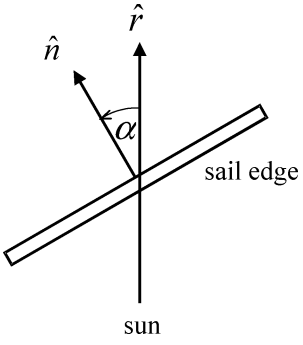

Fig. 1 Solar sail control-angle definition.

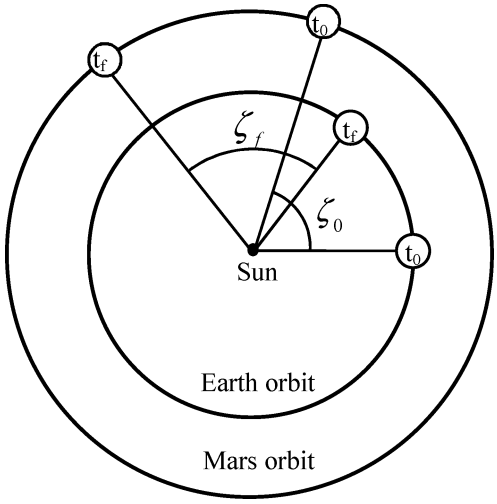

Fig. 2 Initial and final Earth–Mars angular relationships.

Events Model

Compliance of a trajectory with the dynamic constraints indicates its feasibility with respect to the physics, but compliance with pointwise conditions at selected events is also required to ensure that we obtain the desired solution. In a generalized optimal control problem (OCP), events are generalizations of interior point constraints as well as boundary conditions.[8–10] For our problem, the totality of these event conditions can be classified as follows.

Cyclic Conditions

To model the repeating nature of a cyclic trajectory, we constrain the initial and final states of the spacecraft to be equal. Because the Earth and Mars orbits are approximated as circular and coplanar, the problem is simplified in that the initial relative angular position between Earth and Mars (lead angle ζ) may be used to constrain final angular position for a single cycle because planetary distances and velocities are independent of the their inertial angular positions (Fig. 2). The lead angle is determined from the event states as

$$\phi_f = \phi_0 + n_m(t_f - t_0), \qquad \psi_f = \theta_0 + n_e(t_f - t_0)$$

where

$$\phi_0 = \theta_i - n_m(t_i - t_0)$$

and ϕ and ψ are angular positions, or mean anomalies, of Mars and Earth, respectively, and are obtained using their respective mean motions (n_m and n_e). Subscripts 0, i, and f represent initial, intermediate, and final conditions at Earth, Mars, and Earth, respectively. The Earth–Mars lead angle at initial and final times are

$$\zeta_0 = \phi_0 - \psi_0, \qquad \zeta_f = \phi_f - \psi_f$$

Initial and final relative angular positions are constrained by

$$\cos(\zeta_f - \zeta_0) = 1 \tag{4}$$

which is equivalent to

$$\zeta_0 = \zeta_f - 2\pi N_\zeta, \qquad N_\zeta = 0, 1, 2, \ldots \tag{5}$$

Equation (4) is preferable to Eq. (5) because it does not contain the integer N_ζ as an additional decision variable. The cyclic end condition for the spacecraft radial distance is expressed simply as

$$r_0 = r_f \tag{6}$$

Initial and final velocities are also constrained to be cyclic and will be addressed later. The final time t_f remains a free variable in the

optimal control problem. Because of the condition given by Eq. (4), however, the solution must yield the Earth–Mars synodic period (approximately 2.135 years) to be valid.

Swingby Conditions

Force imparted by the solar sail shapes the path between planetary encounter events, but gravity-assist maneuvers at these events drive the form of the whole cycler trajectory. To model the swingby events, velocity discontinuities are employed at the planet's radial distance in the heliocentric frame (sometimes called the "zero-sphere-of-influence patched conic" (Ref. 13, pp. 359–379) or matched asymptotes model). It is assumed that the interaction time with the subject planet is negligibly small in comparison to the total cycle time. The velocity changes direction such that relative to the sun

$$\boldsymbol{V}^+ = \boldsymbol{V}^- + \Delta\boldsymbol{V} \tag{7a}$$

and relative to the planet

$$\boldsymbol{V}_\infty^+ = \boldsymbol{V}_\infty^- + \Delta\boldsymbol{V} \tag{7b}$$

where $\boldsymbol{V}_\infty = \boldsymbol{V} - \boldsymbol{V}_p$ and the superscripts indicate before $(-)$ or after $(+)$ a swingby of a planet moving at velocity $\boldsymbol{V}_p$ relative to the sun. The position states r and θ are constrained to be continuous at both Earth and Mars encounter events:

$$r^- = r^+, \qquad \theta^- = \theta^+ \tag{8}$$

The $\Delta\boldsymbol{V}$ due to the swingbys are optimally chosen by virtue of the problem formulation, but they must be properly constrained. Constraints on the velocity changes are most easily imposed using the planet frames where inbound and outbound velocity magnitudes are equal just before and after a planet encounter forming the event condition:

$$\left|\boldsymbol{V}_\infty^-\right| = \left|\boldsymbol{V}_\infty^+\right| = \boldsymbol{V}_\infty \tag{9}$$

where V_∞ is the hyperbolic excess speed. The velocity direction change is expressed in the planetary frame using the turn angle δ, which exists in the region shown in Fig. 3. Velocities before and after a swingby event in the planet frame are coupled by the cosine of the turn angle:

$$\cos\delta = \left(\boldsymbol{V}_\infty^- \cdot \boldsymbol{V}_\infty^+\right)\Big/ V_\infty^2 \tag{10}$$

The spacecraft undergoes a direction change during the interaction that is restricted by V_∞ and the permissible hyperbolic periapse distance D from the center of the subject planet. This restriction is expressed by (Ref. 13, p. 383)

$$\sin\left(\frac{\delta}{2}\right) = \frac{1}{\left(V_\infty^2/w^2\right)D + 1}, \qquad D_{\min} \le D \le D_{\max} \tag{11}$$

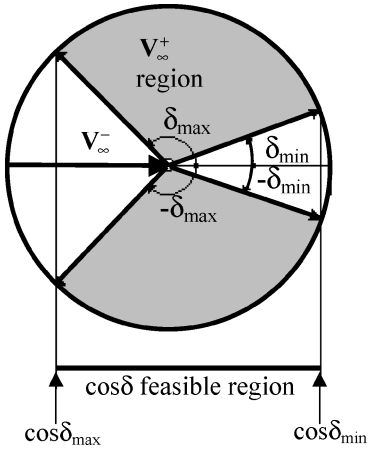

Fig. 3 Constraint on the gravity-assist turn angle δ.

where w is the circular orbit speed at the surface of the planet and D is nondimensionalized by the radius of the planet. Equations (10) and (11) limit the achievable change in velocity direction $\Delta\boldsymbol{V}$ due to the swingbys at Mars and Earth. Design limitations include a selected $D_{\min}$ that is well above the atmosphere where drag effects are negligible and a $D_{\max}$ such that the encounter occurs close enough to the planet to execute a desired task. For a given V_∞, the turn angle is maximum when $D = D_{\min}$ and minimum when $D = D_{\max}$. Substituting these values into Eq. (11) and solving for δ as a function of V_∞ provides an expression for $\delta_{\max}$ and $\delta_{\min}$, respectively. To limit deflections in both the positive and negative directions (Fig. 3), we simply bound the in-track component of V_∞^+. When Eq. (10) characterizes the instantaneous change in path direction and Eq. (11) provides the limits, the boundary conditions are expressed at Earth and Mars events as

$$\cos\delta_{\max} \le \cos\delta \le \cos\delta_{\min} \tag{12}$$

Initial Earth Orbit Departure Condition

Velocity constraints at Mars and Earth have identical form; however, the initial velocity magnitude at Earth has an additional limitation based on available departure rocket capability. Because the sail's journey starts at Earth, the initial conditions are bounded by the maximum available V_∞ from the launch vehicle. Presumably an impulsive burn is used to start the solar sail craft on its cycler trajectory, and so the initial velocity relative to Earth $V_\infty|_{\text{Earth}}$ is restricted. The magnitude of $V_\infty|_{\text{Earth}}$ is limited by a maximum allowable velocity change at $t = 0$ provided by a kick motor, ΔV_{allow}, which provides another boundary condition:

$$0 \le |\boldsymbol{V}_\infty|_{\text{Earth}}| \le \Delta V_{\text{allow}} \tag{13}$$

The direction of $V_\infty|_{\text{Earth}}$ is driven by the OCP and is limited only by the allowable turn angle at each Earth swingby.

Phasing Condition

Finally, phasing the spacecraft with Earth at the end of a cycle is considered. Earth encounter events are constrained to ensure that the sail trajectory intersects Earth's orbital path at precisely the time that the planet is at that same location. The circular orbit assumption is particularly useful for ensuring proper phasing of events because the angular position of a planet is a linear function of time. The final angular position of the spacecraft is constrained by the angular position of the Earth and may be expressed as

$$\cos(\theta_f - \psi_f) = 1 \tag{14}$$

Having established the solar sail's physical, dynamic, and events models, we can set up the OCP as defined in the next section.

Problem Formulation

To transfer payload between the cycler vehicle and the planet's surface, it is presumed that a taxi vehicle residing in a Mars parking orbit will rendezvous and dock with the passing cycler craft and make the trips to and from the surface. If we consider a circular taxi parking orbit, then minimizing the taxi propellant expended in performing the rendezvous every synodic period entails minimizing the ΔV required to join the hyperbolic path of the cycler craft. Using energy relations, this velocity change, ΔV_{taxi}, is

$$\Delta V_{\text{taxi}} = \sqrt{2v_c^2 + V_\infty^2} - v_c$$

where v_c is the circular parking-orbit speed. When this simple model is used for a taxi in a fixed parking orbit, minimizing the taxi propellant is tantamount to minimizing the V_∞ at Mars. In this analysis, the solar sail cycler OCP is constructed using the spacecraft V_∞ at Mars ($V_\infty|_{\text{Mars}}$) as the cost function. Thus, we write the OCP as follows.

Minimize the cost functional:

$$J[\boldsymbol{x}(\cdot), \alpha(\cdot), t_0, t_i, t_f] = V_\infty|_{\text{Mars}} \tag{15}$$

subject to the dynamic constraints given by Eq. (3), the periodicity constraints given by Eqs. (4) and (6), continuity condition [Eq. (8)], swingby effects [Eqs. (9) and (12)], Earth orbit departure limitations [Eq. (13)], and phasing [Eq. (14)]. In addition, the controls are bounded by Eq. (2), which reflects the reality of a one-sided sail. Finally, the states are bounded only to ensure that singularities are avoided in the dynamics, (that is, $r > 0$).

The problem is solved using DIDO,[11] a MATLAB® implementation of the pseudospectral knotting method.[8–10] DIDO incorporates many of the recent advances in the pseudospectral knotting method, including an automatic pattern generation and exploitation of the discrete Jacobian sparsity by way of the nonlinear programming solver SNOPT.[14] To use DIDO, no knowledge of the pseudospectral knotting method is necessary. The optimal control problem is coded in much the same way as one writes it down, thanks to the era of object-oriented programming. Thus, the problem as posed here is almost identical to the way it is coded. The necessary conditions of optimality are automatically satisfied as a result of the covector mapping theorem, the details of which are elaborated in Ref. 10.

Results

The radial parameters for a single Earth–Mars in astronomical units (AU) cycle are

$$r_0 = r_f = 1, \qquad r_i = 1.524$$

The parameters that constrain the path deflections at the events are the maximum allowable ΔV at the initial Earth orbit departure (ΔV_{allow} in nondimensional units), and the minimum and maximum periapse pass distances at Earth and Mars:

$$\Delta V_{\text{allow}} = 0.2(\sim 6 \text{ km/s})$$

$$D_{m\,\min} = 1.06R_m, \qquad D_{m\,\max} \to \infty$$

$$D_{e\,\min} = 1.16R_e, \qquad D_{e\,\max} = 10R_e$$

To restrict solutions to those that pass reasonably close to Earth for docking operations, $D_{e\,\max}$ was chosen to be 10 Earth radii. With this data, the solution is shown in Figs. 4–7 and is validated as follows.

Validating the Output

The time required to complete a cycle was found to be 2.135 years, the Earth–Mars synodic period. As noted earlier, this self-check is a first and crucial validation of the output. Further validation of the results is demonstrated in Figs. 4 and 6. The symbols in these figures are the output from DIDO. The solid lines, which appear to pass through the symbols, are obtained by propagating [with the MATLAB Runge–Kutta ordinary differential equation (ODE) solver ode45] the initial conditions using the DIDO-generated control history (Fig. 5) and the instantaneous velocity changes associated with the gravity assist. It is apparent from Figs. 4 and 6 that there is good agreement between the two solutions. The percentage difference between the DIDO solution and the propagated solution is shown in Table 1 for a few critical parameters because the plots can easily mask large errors. The small differences indicated in Table 1 show the relative validity of the solutions.

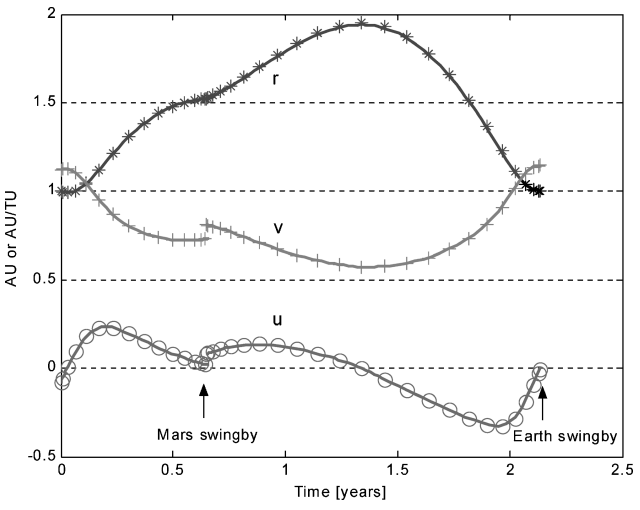

Fig. 4 States obtained from DIDO solutions (symbols) and the propagated solution (lines).

Table 1 Error between final and initial conditions of the propagated path of radial distance r, Mars lead angle ζ, and velocity magnitude V

Trajectory parameter	Final value	Initial value	% Error
r	1.0053	1.000	0.53
ζ	0.6525	0.6512	0.20
V	1.1249	1.1256	0.06

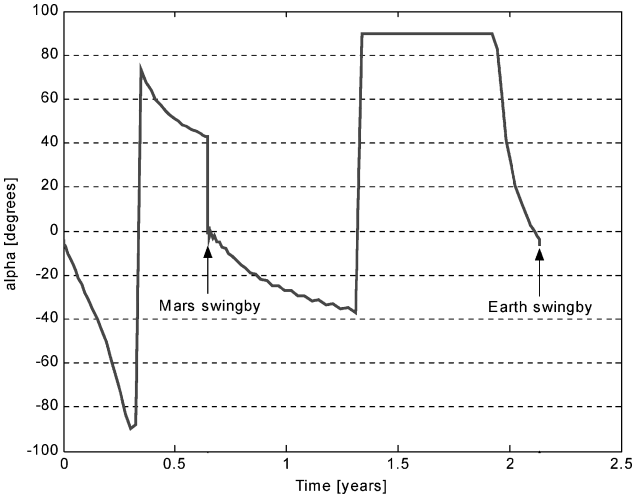

Fig. 5 Optimal control angle α vs time.

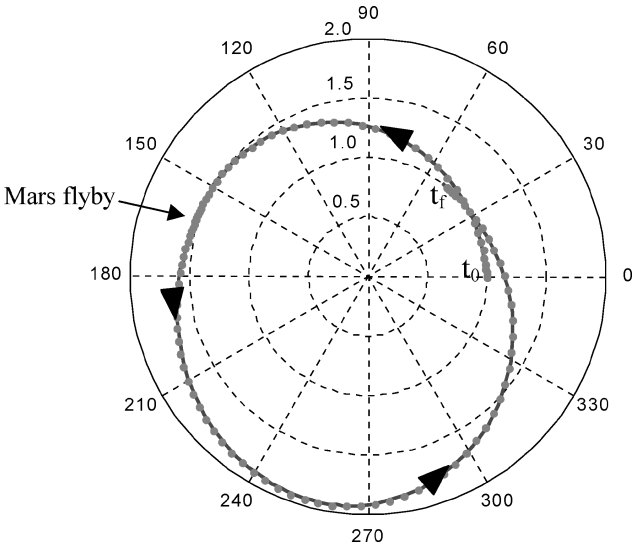

Fig. 6 Comparison of DIDO-generated path (depicted at node points) and propagated path (line).

Discussion of the Output

It is apparent from Figs. 4 and 5 that jumps in the control angle and the free ΔV due to gravity assists are adequately represented by the knotting method, particularly near planetary encounters (Fig. 6). The symbols shown in Fig. 6 represent node points optimally chosen for the OCP solution and are not separated by equal time steps. The

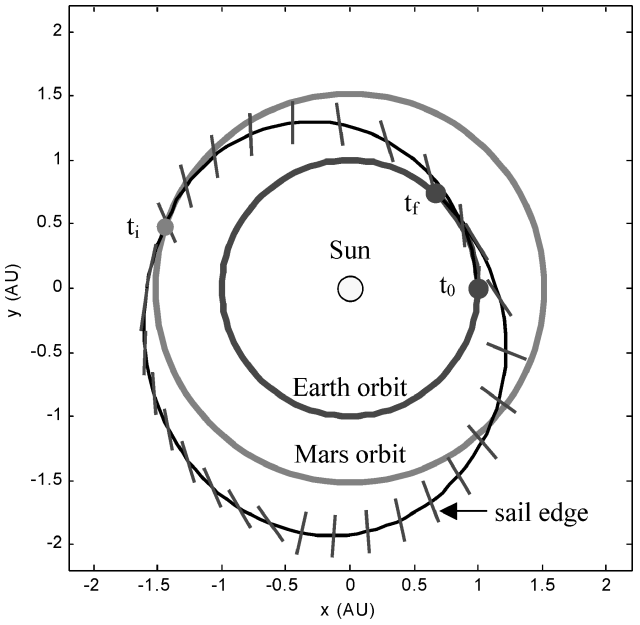

Fig. 7 Single-cycle trajectory with sail orientation.

density of node points near the planets is higher (as a result of the pseudospectral knots) enabling higher resolution representations at exactly those locations most desirable for a closer look.

A quick glance at the state history in Fig. 4 reveals that the spacecraft sails from 1 AU out to Mars's orbit at 1.524 AU and then returns to Earth. A discontinuity in both velocity states occurs at 1.524 and 1 AU representing Mars and Earth swingbys, respectively. The optimal path makes use of large gravity-assist maneuvers (in the planet frame) during planet encounters because of slow hyperbolic excess speeds. The spacecraft initially accelerates in the radial direction (Fig. 4) while decelerating in the transverse direction. At the appropriate time, the sail rotates to an attitude (Fig. 7) that favors more and more positive transverse acceleration to intercept Mars with the lowest V_∞ to minimize the cost function while setting up for the swingby event initiating the return trip. Following Mars swingby, the spacecraft sweeps out to nearly 2 AU (Fig. 6) to ensure proper phasing for Earth intercept. Sail attitude gradually reaches a maximum negative transverse acceleration profile ($\alpha = -35$ deg), then shuts off and follows a ballistic path as it presents an edge aspect to the sun ($\alpha = 90$ deg). The sail trajectory with Earth and Mars encounters is shown in Fig. 7. A similar gravity assist is accomplished at the Earth encounter, and because cyclic end conditions were imposed, the same control profile will reproduce the trajectory repeatedly. Because of these constrained end conditions, the initial Earth departure hyperbolic excess velocity only required 4.3 km/s, not the maximum allowable limit of 6 km/s.

A noticeable difference between the solar sail cycler and the traditional Aldrin cycler using impulsive burns is the large swingby angular deflections with respect to Mars and Earth. Because the Aldrin cycler minimizes propellant mass, it resides in a natural Keplarian orbit most of the time. As such, it tends to have large V_∞ at Mars and Earth, thus, restricting turn angles. The solar sail, on the other hand, can change orbital energy with no direct impact to the cost function and achieve low hyperbolic excess speeds that permit large turn angles. The results of this analysis show that a 75-deg Mars turn angle and a 29-deg Earth turn angle provide the optimum path. Interestingly, the sail never goes down to the minimum allowable periapse distance with Mars to achieve a bigger swingby deflection. Furthermore, the sail swings by Earth at the maximum allowable perigee distance, not the minimum allowable distance. Table 2 summarizes the cycler characteristics.

The moderately high-performance sail used in this analysis ($\beta = 0.17$) permits a very attractive Mars approach speed; however, in designing a cycler mission, it is useful to know what optimal mission profiles exist for a range of sail performances. For example, one

Table 2 Earth–Mars solar sail cycler planetary swingby parameters

Planet	V_∞, km/s	D, planet radii	δ, turn angle, deg	Time to planet, months
Mars	2.53	1.27	75	7.7
Earth	4.30	10.00	29	18.0

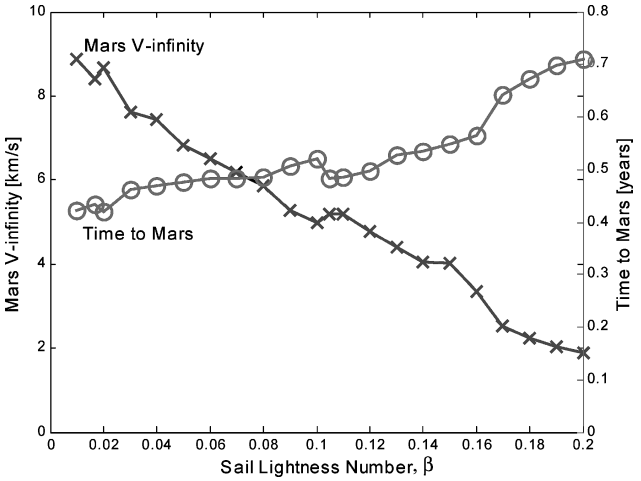

Fig. 8 Effect of varying sail performance β on a cycler.

might desire to launch the same payload in the near future with a less capable sail. Substituting various sail performance parameters in Eq. (3) results in the trajectory characteristics shown in Fig. 8. The higher-performance sails tend to take a longer time to reach Mars to reduce V_∞ at Mars. As the sail performance is reduced to $\beta = 0.01$, the cycler flyby characteristics look more like an Aldrin cycler.

Conclusions

The cycler problem can be posed as a periodic OCP with interior point constraints and jump discontinuities. Solar sails permit more flexibility in mission design for Earth–Mars cyclers by alleviating the large V_∞ near planetary encounters. Solar sails also have the usual advantage over mass-ejection propulsion systems in that they provide an almost inexhaustible supply of propulsive energy. This point is essential to the use of cyclers because they are expected to visit planets periodically and almost indefinitely.

Acknowledgments

This research was sponsored in part by the Jet Propulsion Laboratory (JPL) and the Naval Postgraduate School. We gratefully acknowledge the strong and sustained support of Steven E. Matousek of JPL, without which this project would never have been completed. We also thank Dennis Byrnes and Jon Sims, also of JPL, for providing valuable insights to this problem; in particular, their suggestion of using the hyperbolic speed for the cost function was vital to the proper formulation of the problem posed earlier by I. M. Ross.

References

[1]Byrnes, D., McConaghy, T., and Longuski, J., "Analysis of Various Two Synodic Period Earth-Mars Cycler Trajectories," AIAA Paper 2002-4423, Aug. 2002.

[2]McConaghy, T., Longuski, J., and Byrnes, D., "Analysis of a Broad Class of Earth–Mars Cycler Trajectories," AIAA Paper 2002-4420, Aug. 2002.

[3]Chen, J., Landau, D., McConaghy, T., Okutsu, M. O., Longuski, J., and Aldrin, B., "Preliminary Analysis and Design of Powered Earth–Mars Cycling Trajectories," AIAA Paper 2002-4422, Aug. 2002.

[4]Byrnes, D., Longuski, J., and Aldrin, B., "Cycler Orbit Between Earth and Mars," *Journal of Spacecraft and Rockets*, Vol. 30, No. 3, 1993, pp. 334–336.

[5]Niehoff, J., "Pathways to Mars: New Trajectory Opportunities," American Astronautical Society, AAS Paper 86–172, July 1986.

[6]McInnes, C. R., *Solar Sailing: Technology, Dynamics and Mission Applications*, Praxis, Chichester, England, U.K., 1999.

[7]Coverstone, V. L., and Prussing, J. E., "Technique for Escape from Geosynchronous Transfer Orbit Using Solar Sail," *Journal of Guidance, Control, and Dynamics*, Vol. 26, No. 4, 2003, pp. 628–634.

[8]Ross, I. M., and Fahroo, F., "Pseudospectral Knotting Methods for Solving Optimal Control Problems," *Journal of Guidance, Control, and Dynamics*, Vol. 27, No. 3, 2004, pp. 397–405.

[9]Ross, I. M., and Fahroo, F., "A Direct Method for Solving Nonsmooth Optimal Control Problems," Proceedings of the International Federation of Automatic Control, 15th World Congress, Barcelona, July 2002.

[10]Ross, I. M., and Fahroo, F., "Discrete Verification of Necessary Conditions for Switched Nonlinear Optimal Control Systems," Proceedings of the American Control Conf., Invited Paper, Boston, June 2004.

[11]Ross, I. M., and Fahroo, F., "User's Manual for DIDO 2002: A MATLAB Application Package for Dynamic Optimization," Dept. of Aeronautics and Astronautics, Naval Postgraduate School, NPS TR AA-02-002, Monterey, CA, June 2002.

[12]Bryson, A. E., *Dynamic Optimization*, Addison Wesley Longman, Reading, MA, 1999, pp. 184, 185.

[13]Bate, R. R., Mueller, D. D., and White, J. E., *Fundamentals of Astrodynamics*, Dover New York, 1971.

[14]Gill, P. E., Murray, W., and Saunders, M. A., "SNOPT: An SQP Algorithm for Large-Scale Constrained Optimization," *SIAM Journal on Optimization*, Vol. 12, No. 4, 2002, pp. 979–1006.

C. Kluever
Associate Editor